High Data-Rate OESCLU-Band Transmission

Benjamin J. Puttnam, *Member, IEEE,* Ruben S. Luís, *Senior Member, IEEE,* Ian Phillips, *Member, IEEE,* Mingming Tan, *Member, IEEE,* Aleksandr Donodin, *Member, IEEE,* Dini Pratiwi, *Member, IEEE,* Lauren Dallachiesa, Member, IEEE, Yetian Huang, *Member, IEEE,* Daniele Orsuti, *Member, IEEE,* Divya Ann Shaji, Student *Member, IEEE,* Mikael Mazur, Member, IEEE, Nicolas K. Fontaine, *Senior Member, IEEE,* Haoshuo Chen, *Member, IEEE,* Dicky Chung, *Member, IEEE,* Victor Ho, *Member, IEEE,* Budsara Boriboon, G. Rademacher, Senior Member, IEEE, Cristian Antonelli, *Member, IEEE,* Luca Palmieri, *Member, IEEE,* Ray Man, *Senior Member, IEEE,* Roland Ryf, *Fellow, IEEE,* David T. Neilson, *Fellow, IEEE,* Wladek Forysiak, *Member, IEEE* and Hideaki Furukawa, *Member, IEEE.*

***Abstract*—We combine 6 doped-fiber amplifiers (O-(x2), E-, S-, C-, L-bands) with discrete Raman U-band amplifiers and distributed Raman-amplification to transmit in each of the low-loss transmission bands of a standard optical fiber. For transmission distances up to 100 km, we explore ultra-wideband transmission of up to 1505 x 25 GHz spaced channels covering the O-, E-, S-, C-, L- and U-bands from 1281.2 nm to 1649.9 nm. After describing the amplifier and spectrum flattening technology, we first characterize the transceiver in back-to-back configuration. Then, for 50 km transmission, we report a record aggregate transmission bandwidth of 37.6 THz with a data-rate of 402.2 Tb/s, estimated from GMI, and 378.9 Tb/s after FEC decoding. 100 km transmission allows a 36.6 THz bandwidth with 339 Tb/s GMI estimated data-rate and 322.8 Tb/s decoded data-rate. These results show the potential of ultra-wideband transmission covering the low-loss window of silica fibers as well as the challenges of building such system on longer fiber spans.**

***Index Terms*—Wideband transmission, Multi-band transmission, Raman amplifier, Optical amplifiers**

I. INTRODUCTION

Increasing demand for high data-rate optical transmission [1-2] has driven investigation of both additional spectral windows [3-4] and new fibers utilizing the spatial domain [5-6]. Of these approaches, adopting new transmission windows also offers the potential benefit of prolonging the life of deployed optical fibers [4] to provide additional transmission capacity without the need for new fiber deployment. The recent maturing of hollow core fiber technology with broadband transmission potential further encourages development of wideband amplification and component eco-systems [7].

However, moving away from the low-loss 1550 nm region of standard fibers requires development of amplification schemes to complement the erbium (E-) doped fiber amplifiers (DFAs) that are the staple of C- or C+L-band transmission systems. C+L-band system have shown multi-span throughputs above 120 Tb/s [8] and up to 150 Tb/s for single-span transmission

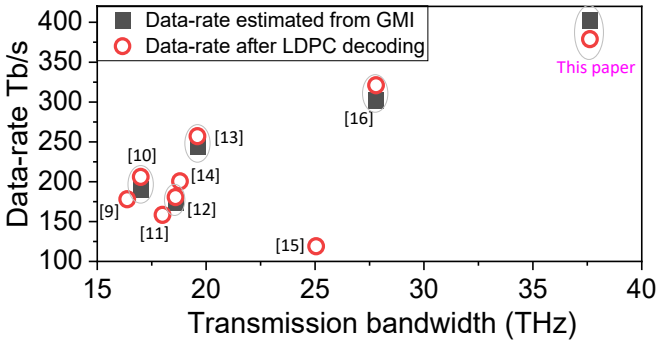

Fig. 1: Wideband (> 15 THz) transmission demonstration exceeding 100 Tb/s in SMF [9-16, 18]

[13]. In addition to EDFAs, SCL-band systems have used thulium (T-) DFAs, semiconductor optical amplifiers (SOAs) as well as distributed and discrete Raman amplification [9-15]. This has enabled data-rates up to 256 Tb/s utilizing 20 THz bandwidth [14] and 200 Tb/s transmission over 2 x 100 km spans [15]. More recently, wider-band transmission demonstrations have used bismuth (B-) DFAs for O-band and discrete Raman amplifiers for U-band channels, achieving 119 Tb/s over OSCLU-bands with a cumulative bandwidth of 25 THz in a deployed 45 km fiber [16]. E-band BDFAs were also used with distributed Raman amplification for ESCL-band transmission over 27.8 THz with >320 Tb/s data-rate over 50 km fiber [17] and >270 Tb/s over 2 x 100 km spans [18].

Here, we expand on the results presented in [19, 20] investigating DWDM transmission in each of the primary transmission bands of the low-loss window of standard optical fibers. This is done by constructing a transmission system using a combination of 6 DFAs, including praseodymium (P-) DFAs for O-band, together with O- and E-band BDFAs, TDFAs and C/L EDFAs with both discrete Raman (U-band) and distributed Raman amplification. We first characterize the amplifiers used

Ben Puttnam, Ruben Luis, Budsara Boriboon, and Hideaki Furukawa are members of the Network System Institute at The National Institute of Information and Communications Technology, 4-2-1 Nukui-Kitamachi, Koganei, Tokyo 184-8795, Japan. (e-mail: ben@nict.go.jp).

Lauren Dallachiesa, Yetian Huang, Nicolas K. Fontaine, Mikael Mazur, Haoshuo Chen, Roland Ryf, and David T. Neilson are with Nokia Bell Labs, 600 Mountain Ave, New Providence, NJ 07974, USA

Ian Phillips, Mingming Tan, Alezandr Donadin, Dini Pratiwi and Wladek Forysiak are with Aston Institute of Photonic Technologies, Aston University, Birmingham, UK,

Dicky Chung, Victor Ho and Ray Man are with Amonics PLC,14F Lee King Industrial Building, Kowloon, Hong Kong.

Georg Rademacher is with the University of Stuttgart, 70174 Stuttgart, Germany.

Daniele Orsuti and Luca Palmieri are with University of Padova, Via G. Gradenigo 6/B, 35131, Padova, Italy.

Divya Shaji and Cristian Antonelli are with University of L'Aquila and CNIT, 67100, L'Aquila, Italy.

and measure the back-to-back transceiver performance. We then report 50 km transmission of 1505 channels with 25 GHz spacing and 16, 64 or 256 dual-polarization (DP-) quadrature-amplitude modulation (QAM) at 24.5 GBaud [19]. This leads to an aggregate transmission bandwidth of 37.6 THz and generalized mutual information (GMI) estimated data-rate of 402 Tb/s. We then extend the transmission distance to 100 km [20] before comparing the achievable throughputs in each band.

For context, Fig. 1 shows a summary of recent single-span, high data-rate wideband transmission demonstrations with >15 THz bandwidth and more than 100 Tb/s data-rate. The 50 km experiment presented here exceeds the previous highest single-mode fiber (SMF) data-rate [17] by over 25% with the transmission bandwidth increasing by 35%. These demonstrations show the challenges of high fiber loss in the new transmission bands, but also show that OESCLU-band multi-band transmission may be suitable for high data-rate transmission over a range of distances suitable for a diverse range of networking scenarios.

II. Description of Amplifiers and Spectrum Shapers

The transmission set-up is fully described in section III with this section first outlining the key sub-systems and the amplification strategy that provide a deeper understanding of the transmission results present in Section IV. A combination of 6 variants of DFAs cover O- to L-bands with discrete Raman amplifiers for U-band and additional distributed Raman amplification used to enable transmission of OESCLU-band signals. As with a previous exploration of ESCL-band transmission [21], EDFAs were used for C and L-band amplification, with TDFAs used for S-band amplification. E-band amplification was achieved in germanium-co-doped BDFAs. The EDFAs had a typical noise figure (NF) of 5 dB in C-band and 6 dB in L-band. EDFAs with 13 to 22 dBm output power were used for test-channels and high power (up to 27 dBm) used for full-band WDM amplification. C-band amplifiers provided gain from around 1527 nm to 1568 nm. L-band amplifiers were optimized for extended long-wavelength performance being based on 3 DFA stages similar to [22], providing gain from 1569 nm to 1623 nm with the doped-fiber design based on that described in [23]. All erbium DFAs used a silica glass host. The S-band TDFAs contained thulium-doped fluoride fibers [24] to provide gain from 1465 nm to 1524 nm. The NF was < 7 dB for all wavelengths with full wavelength dependant NF measurements available at [25].

A. BDFAs for O and E-band

In addition to germanium-co-doped BDFAs used for E-band gain, phosphorous co-doped BDFAs were also used for O-band amplification. Both DFAs used silica as the glass host. The characteristics of both BDFA variants are shown in Fig. 2. Both had a similar noise figure between 5 and 6 for single wavelength 0 dBm input signals, with measurements ranging from 1425 nm to 1465 nm for E-band BDFA (E-BDFA), and 1280 nm to 1330 nm for the O-band BDFA (O-BDFA). The E-BDFA had a higher output power reaching up to 25 dBm whilst the O-BDFA gave around 21 dBm output power. Although not utilized here

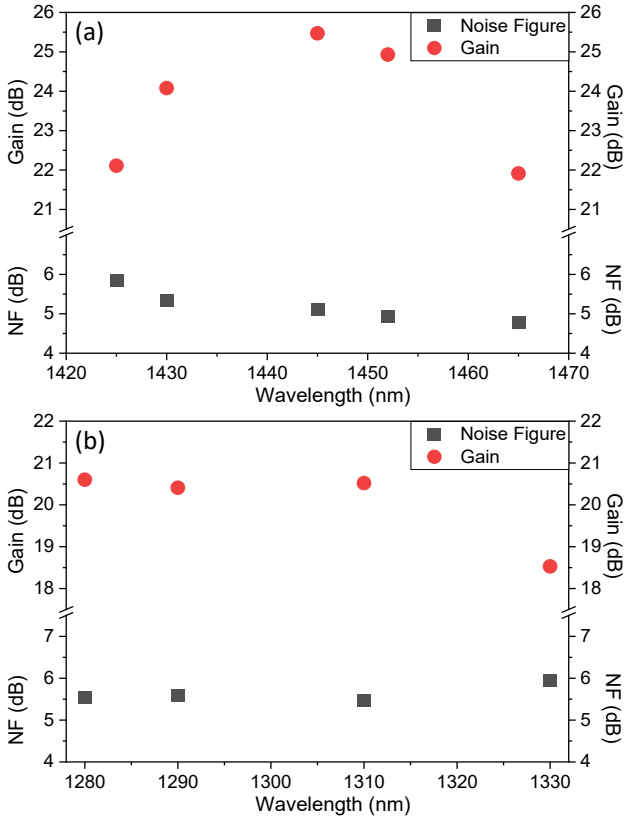

Fig. 2: Measured gain and noise figure with 0 dBm single wavelength input signals for (a) E-BDFA and (b) O-BDFA

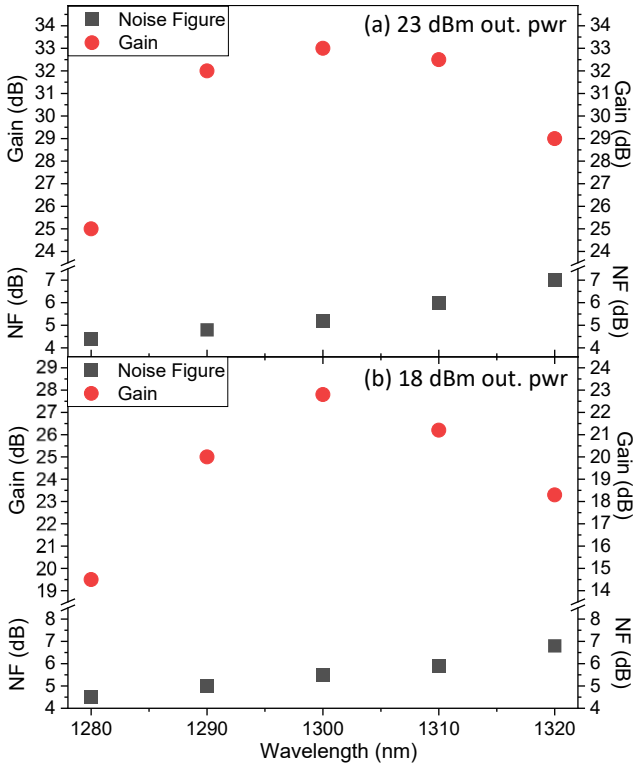

Fig.3: Measured gain and noise figure for -10 dBm single wavelength input signals for (a) 23 dBm output power PDFA and (b) 18 dBm output power PDFA for O-band signals

due to the large separation between O and E-band optical processor (OP) ranges and to the desire to maintain high power-per-channel at the amplifier outputs, we note that BDFAs covering both O- and E-bands have been reported [26-28]. The characteristics of each amplifier were tailored depending on whether they were intended for single channel operation in transmitter/receiver or for DWDM amplification but contained more than 100m fiber in both cases. In both O and E-band polarization maintaining (PM) SOAs were also used in the test-band to compensate for the increased modulator loss in these bands in the absence of additional DFAs. The SOAs had NF <7 dB and around 15 dBm output power.

B. O-band PDFAs

Due to a limited number of BDFAs in the O-band region, O-band amplification was also achieved with praseodymium (P-) DFAs with 2 variants giving output powers of 18 dBm or 23 dBm. The key differences between the two variants were the length of the fluoride doped fiber and the maximum pump currents. The gain and NF of the 2 PDFA varieties with -10 dBm input signals are shown in Fig. 3. The overall gain spectrum is narrower than the O-BDFAs with the NF also slightly higher varying from just over 4.5 dBm at 1280 nm to around 7 dB at 1320 nm. There is a strong wavelength dependant gain with the 1320 nm channel gain measured to be 8 dB lower than 1300 nm channel in both amplifier variants.

C. U-band discrete Raman amplifiers (DRAs)

U-band amplification was achieved in a set of discrete Raman amplifiers pumped with shaped amplified spontaneous emission (ASE). The amplifiers were based on the design in [29] and described in more detail in [30]. Based on availability, a combination of 3 distinct Raman gain fibers were used: 1 km highly nonlinear fibre (HNLF) with ~1 dB insertion loss, two separate amplifiers, each with an 8 km span of inverse dispersion fibre (IDF) with ~3 dB loss, and 0.51 km highly nonlinear dispersion-shifted fiber (HNLDSF) with ~1.5 dB loss. Figure 4(a) shows a schematic diagram of the proposed U-band DRA. A conventional C-band EDFA was used as the ASE seed source for the pump. A band-pass optical filter was used to control bandwidth and center wavelength of the ASE pump, which was found to provide maximum amplifier gain at around 1535 nm with around 3 nm bandwidth. The shaped ASE was then amplified by a high power EDFA and fed into the signal-pump combiner from a backward-propagating direction, to minimise RIN transfer [31]. The ASE pump also minimised RIN transfer by ensuring no coherent interaction between the pump and the signal [32].

As particularly noticeable in the long IDF, Rayleigh backscattering as well as reflections from passive components led to unstable random lasing above certain pump power thresholds. For this reason, the pump powers for each amplifier were determined by the maximum allowable power for stable operation and being 2W, 1.6 W, and 2.1 W for HNLF, IDF and HNLDSF respectively.

Figure 4 (b) shows the net gain and NFs for the HNLF based amplifier for 3 different input powers. The gain variations

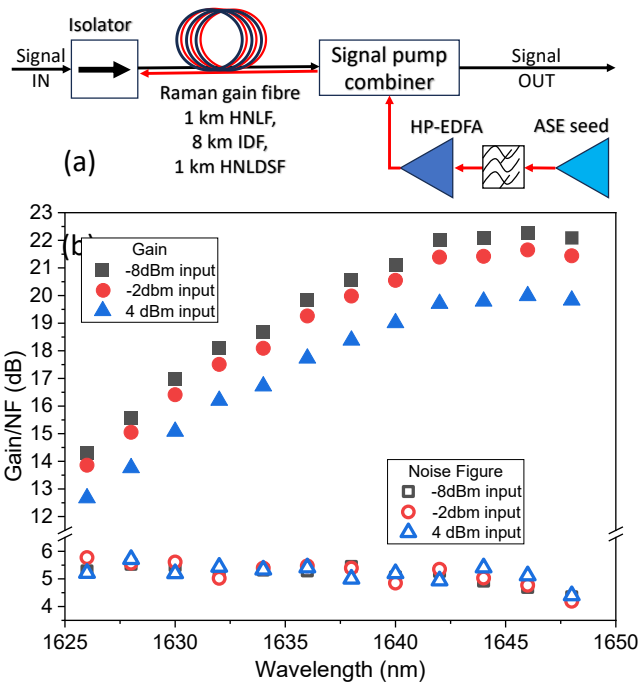

Fig. 4: (a) Configuration of discrete Raman amplifiers (DRA) (b). Measured net gain and noise figures of U-band DRA based on 1km HNLF

across the utilised 25 nm spectrum were ~8 dB and similar for each of the DRAs. For an input power of -8 dBm, using 1km HNLF gave the highest net gain of 22.3 dB at 1646 nm. The 0.51 km HNLDSF gave 21 dB gain, which reduces to 13 dB at 1625 nm, whilst the 8km IDF had a maximum gain of 16.2 dB reducing to 8dB at 1625nm [33]. The highest gain achieved with the HNLF was due to the higher Raman gain coefficient and comparatively lower loss. The net gain was decreased to 20 dB at 4 dBm input signal power due to the pump depletion. For the same input power, a net gain of 19.6 dB and 13.8 dB was achieved using HNLDSF and IDF, respectively. The lowest NF of 4.2 dB was achieved using 1 km HNLF at 1646 nm, but it increases to 5.8 dB at 1626 nm due to the greater thermal noise generated by the pumps at shorter signal wavelengths [34]. The use of the IDF resulted in a NF of 6.3 dB at 1648 nm due to increased fibre length and lower Raman gain coefficient with the NF increasing to 7.6 dB at 1628 nm. For the HNLDSF, the NF range was 8.1-13.7 dB, significantly higher than other fibre types. This is believed to arise from the zero-dispersion wavelength of this fibre (1548nm), being close to the pump center wavelength that led to additional non-linear interactions and comparatively lower gain than other fibers at comparable pump powers.

D. Optical processors/blockers for O and E-bands

The other notable component of the OESCLU band transmission was spectrum shaping technology used in the E and O-bands, also referred to as an OP, dynamic gain equalizer or blocker. For all the bands, as described in the next section, OPs were used to shape the transmission spectrum and make a notch in the transmitted spectrum to accommodate the test-

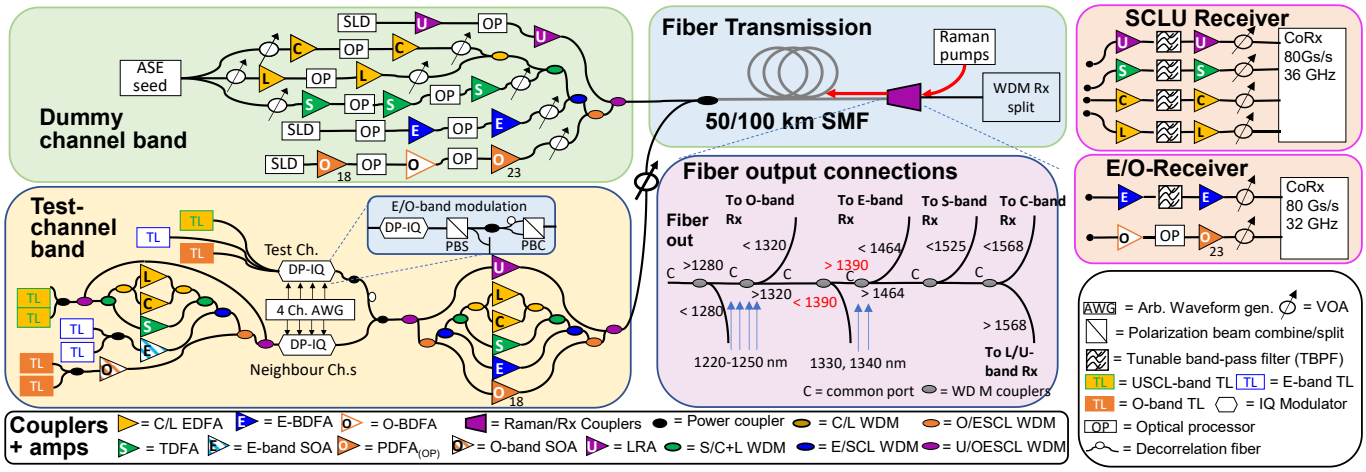

Fig.5: Transmission set-up showing (a) ESCL-band transmitter (b) SCL and E-band receiver set-up, (c) transmission scheme for single-span transmission over 50 km, 100 km and 150 km and (d) transmission for 200 km amplified transmission. Number below PDFA indicates which output ppower variant was used 18 dBm or 23 dBm

channels. The OP was particularly crucial in the O-, E- and U-bands where the BDFAs and discrete Raman amplifiers did not contain gain-flattening filters (GFFs) that were available in the T-, P- and E-DFAs. In the U-band, a commercial wavelength-selective switch, based on liquid crystal on silicon (LCoS) and operating from 1575.8 nm to 1651.3 nm, was used.

The E and O-band spectra were shaped by custom developed multi-port OPs similar to that described in [35]. These were LCoS based devices with multiple individual 1 x 1 ports. The E-band OP had 18 ports operating from 1400 nm to 1465 nm, whilst the O-band device had 16 ports and was capable of covering > 100 nm bandwidth from 1240 nm to 1348 nm. The E-band OP used a transmission grating with a 1.2 µm period originally intended for the O-Band, with the incidence angle rotated to 59 degrees to optimize performance in the E-band. The grating is mounted on a low index glass prism that partially linearizes the spectral dispersion. The optical system consists of front optics that expand the beams and provide required polarization diversity for the grating, LCoS and spectrometer optics that image the dispersed wavelengths onto the LCoS. The minimum loss measured for a single pass of the E-band device was 5 dB but the insertion loss of all ports was observed to increase to around 9 dB after shipping. The loss of O-band device ports used varied between 4 and 6 dB across the wavelength range. The roll-off of the passband edges was approximately 1 GHz/dB for both devices with some variation between wavelength channels.

III. Experiment Description

The experimental set-up, shown in Fig. 5. comprised a sliding 3 channel test band within a wideband WDM signal constructed from shaped amplified spontaneous emission (ASE). The test-band consisted of a test channel between neighbour channels originating from 10 kHz linewidth tunable lasers (TLs) for SCLU-band channels and 200 kHz linewidth TLs for E- and O-band channels. The test and neighbour channels were independently modulated in dual-polarization IQ-modulators (DP-IQ) driven by four arbitrary waveform generators (AWGs) operating at 49 GS/s. These produced 24.5 GBd, DP-QAM root-raised cosine shaped signals with a roll-off of 0.01 based on 2^{16}-1 bit pseudo-random binary sequences. For back-to-back (B2B) and 50 km transmission DP-256QAM was used for SCL-band channels, with DP-64QAM used for E- and U-band signals while DP-16QAM was used for O-band channels. For 100 km transmission, DP-64QAM was used for ESCL- and U-band signals while DP-16QAM was used for O-band channels.

The same modulator type was used for all measurements. However, for E- and O-band modulation, the wavelength dependence of an internal polarization beam splitter (PB-S) severely degraded modulation quality in one polarization. As a result, E- and O-band signals were split in a wideband PBS after modulation with the best polarization further split and combined with a fixed delay (3m patch cord) on one path in a PB combiner (PB-C) to reconstruct a DP signal, shown as an inset in the test-channel band panel of Fig. 5. The modulator loss, shown as a function of wavelength in Fig. 6, varied from 22 dB in C-band to 26.5 dB in U-band, but the total loss including external polarization multiplexing reached almost 28 dB in E-band and 30 dB in O-band.

Dummy wavelength channels were generated from ASE noise [36] shaped using the band-specific OPs and amplifiers described in the previous section. To minimize the required number of DFAs and discrete Raman amplifiers, the U-, E- and O-band noise seeds used high power super-luminescent diodes (SLDs) with 16~18 dBm output power, and less than 4 dB power variation in the transmission band, centered at 1640nm, 1440 nm and 1300 nm respectively. The OPs were used to carve a movable notch in the dummy channel spectrum to accommodate the current test-channel. Commercial LCoS-based OPs were used for USCL-bands, with custom developed multi-port OPs used for E/O-bands, as described in section II.

The combined test and dummy channels were transmitted over 50 or 100 km of suppressed OH-peak SMF with loss of 0.35 dB/km, 0.24 dB/km, 0.19 dB/km and 0.21 dB/km at 1300 nm, 1440 nm, 1560 nm and 1625 nm, respectively. Six counter

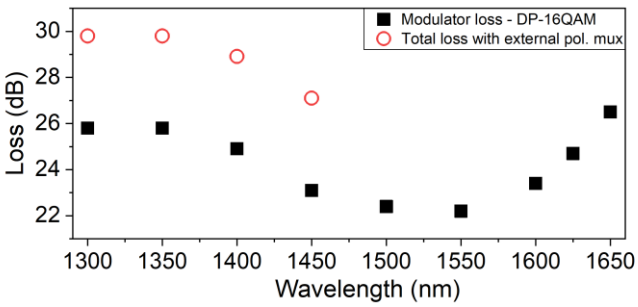

Fig. 6: Modulator loss vs wavelength for 24.5 GBd DP-16QAM modulation and including external polarization multiplexing for E and O-band channels

propagating Raman pumps were injected into the link. Four spaced by 10 nm from 1220 nm to 1250 nm, each with 200 mW power into the fiber, were added below O band channels. Additionally, two pumps with 60 mW into the fiber were added between the O- and E-bands at 1340 nm and 1350 nm. As shown in Fig. 1, the pumps were added in WDM couplers after the fiber, which also separated the per-band signals for reception. The input transmission spectrum was based on a course trial and error optimization to roughly counter the fiber attenuation and stimulated Raman scattering (SRS), except for O-band where the highest achievable power of 20 dBm was used. The total per-band launch powers were 21.5 dBm (E), 20 dBm (S), 17 dBm (C), 17.5 dBm (L) and 18.5 dBm (U), with 1 to 3 dB channel power gradient across bands was used for the 100 km measurement, as shown in Fig. 9 (a). A study of the optimum launch powers in wideband systems can be found in [37].

In each band, the receiver path consisted of amplification stages on either side of a 0.4 nm tunable band pass filter (TBPF) centered on the test-channel with a VOA for power adjustment. In the absence of a programmable filter, an OP was used as the receiver filter for the O-band. For USCL-band signals, a single coherent receiver (CoRx) detected the signal using a 10 kHz linewidth local oscillator (LO). E- and O-band signals each used distinct CoRxs with band-specific hybrid, dual-window photodiodes, and a 200 kHz linewidth LO laser. The signals were acquired by an 80 GS/s real-time oscilloscope that stored traces for offline processing. The throughput of each wavelength channel was estimated both from the GMI and through low-density parity-check code (LDPC) decoding of the received data. The GMI [38, 39] estimated the highest possible data-rate that could be obtained, assuming the availability of the optimal error correction code and sufficient resources, whilst the decoding used the widely available DVB-S2 codes with code puncturing to increase the granularity [40]. The code rate was systematically reduced with the best code-rate to reach a BER $<5\times10^{-5}$ finally selected. The decoded data rate also assumed an additional 1% overhead outer decision code. Signal quality and throughput measurements were performed on three 10 µs traces for each wavelength channel in turn, with the final GMI estimated and decoded data-rates calculated by summing those for all channels received with Q-factor exceeding 2 dB.

IV. Results and Discussion

A. Back-to-back characterization

A B2B transceiver characterizations was performed for each band in turn by connecting the combined test and dummy band signal directly to the appropriate band receiver filter, bypassing the first amplification stage used in the transmission setup. The characterization shows the received signal-to-noise ratio (SNR) and data rate for 250 GHz spaced channels across the transmission bandwidth. We note that no additional noise was added but this was the resulting OSNR from the amplifiers and components in the transceiver path. Figure 7 (a) shows the SNR and Fig. 7 (b) shows the GMI estimated data-rate for the measured channels. We note that the SNR was extracted from the received signals and therefore may also contain a component of non-linear noise. Similar SNRs and data-rates were achieved for the S, C and L-bands with marginally higher SNRs and data-rates achieved in the S-band.

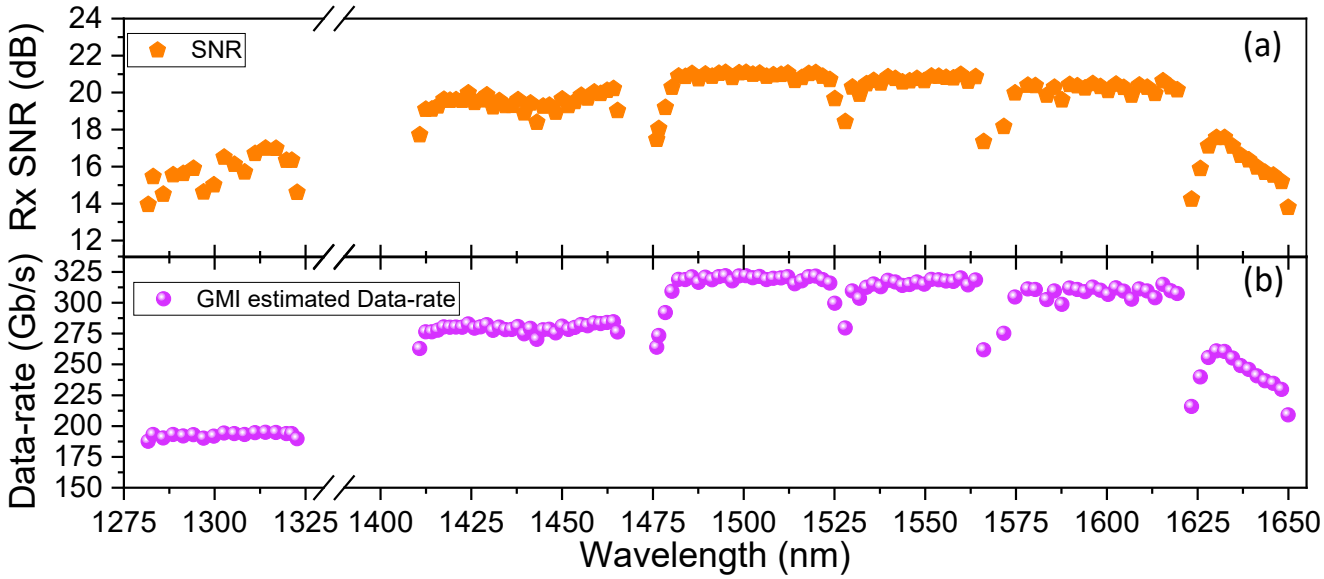

Fig.7: (a) Back-to-back characterization of the received signal-to-noise ratio estimate from Q-factor of roughly 250 GHz spaced channels across OESCL- and U-bands and (b) GMI estimated data-rate of same channels

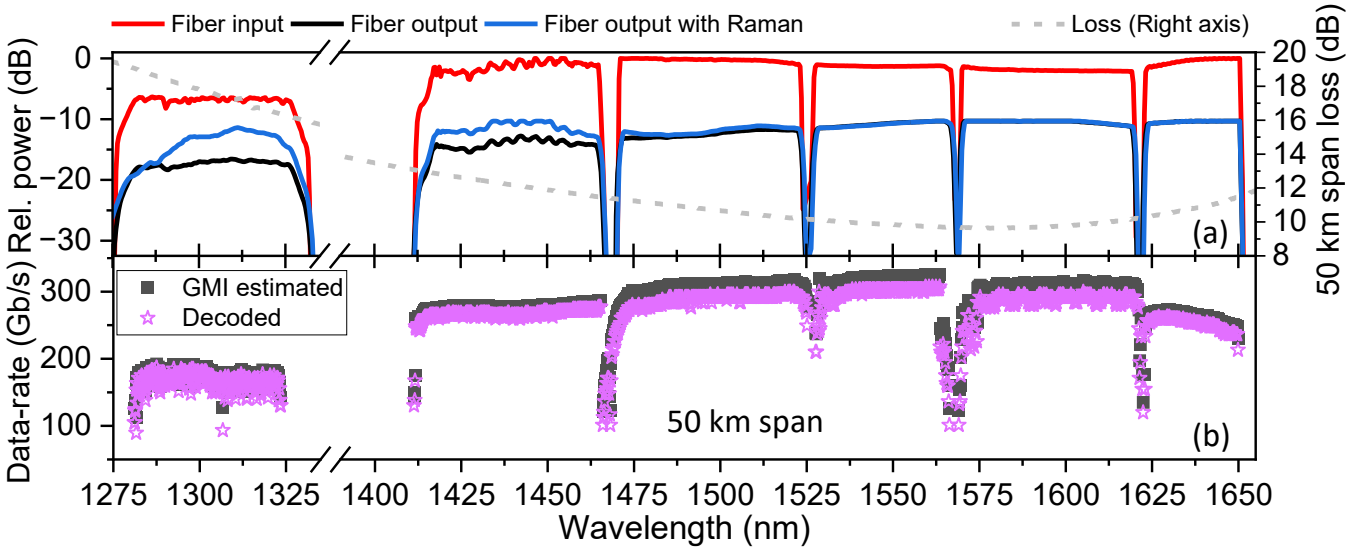

Fig.8: (a) Left-axis - OESCLU-band signal at fiber input (red), output (black) and after Raman amplification (blue) 1 nm res., Right-axis span loss of 50 km fiber (b) GMI estimated and LDPC decoded data-rate after 50 km OESCLU-band transmission

This is attributed to the fact that the S-band dummy channel path contained 2 OPs compared to one for C and L-bands which meant that the extinction ratio of the notch used to accommodate the test channels was higher. This led to marginally higher receiver OSNR at the receiver for the B2B case, without the additional amplifiers needed for fiber transmission. The L-band, in contrast, had slightly reduced OSNR compared to C-band due to the larger number of channels giving slightly lower power per channels and lower noise performance of the high power EDFAs used after the OP. The E-band SNR was further reduced compared to the S, C and L-bands. This is attributed to various factors including the increased post-shipping insertion loss of the OP (which meant it was necessary to amplify between passes), the NF of the BDFA, and the impact of higher modulator loss and insertion loss of the external polarization-multiplexing that significantly reduced the input power to the post-modulator BDFA.

Since all test-channel modulation was carried out in the same modulator type designed for C-band operation, the O-band signals had a particularly high modulation loss (See Fig. 6) and subsequently lower input power to the post modulator amplifiers. In addition, the neighbor channel lasers of the test-band had lower output power despite SOA amplification. This meant that the modulator input power was also lower than the other bands. This is believed to account for the low SNR for O band channels, along with the overall higher loss of passive components in this region and some impact of the semi-manual modulator biasing.

B. A. 50km span transmission

The characteristics of the Raman-amplified 50 km fiber span are shown in Fig. 8 (a). The launched OESCLU-band input signal (red) becomes tilted at the fiber output (black) by the combination of SRS and the fiber loss profile (grey, right-axis). The addition of the

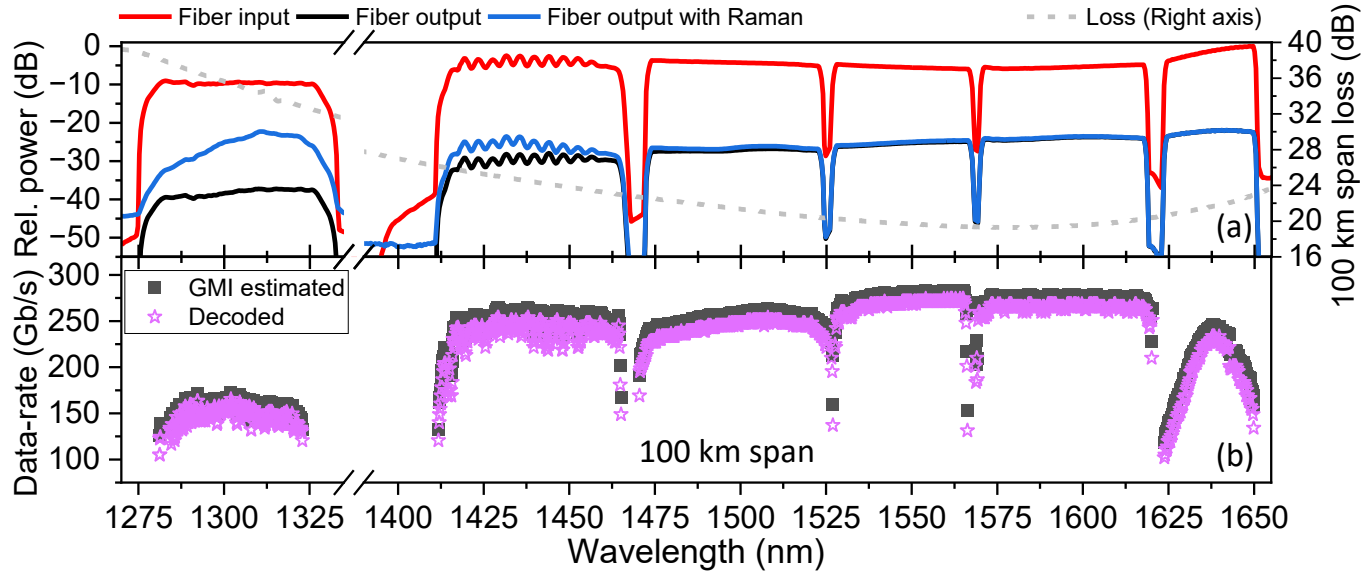

Fig.9: (a) Left-axis - OESCLU-band signal at fiber input (red), output (black) and after Raman amplification (blue) 1 nm res. Right-axis span loss of 100 km fiber (b) GMI estimated and LDPC decoded data-rate after 100 km OESCLU-band transmission

TABLE I
COMPARISON OF 50 KM AND 100 KM TRANSMISSION

Distance \ Band		O	E	S	C	L	U
50 km	No. Channels	302	314	318	195	253	123
	B'width (THz)	7.6	7.9	8.0	4.9	6.3	3.1
	GMI data-rate (Tb/s)	52.3	86.6	95.1	60.2	75.9	32.1
100 km	No, Channels	275	310	296	195	245	119
	B'width (THz)	6.9	7.8	7.4	4.9	6.1	3.0
	GMI data-rate (Tb/s)	42.9	76.4	74.6	53.9	67.1	24.1
% decrease-per-band		**21.9**	**13.4**	**27.5**	**11.7**	**13.1**	**33.2**

Raman pumps provides only moderate gain in the 50 km fiber, reaching around 6 dB in O-band and 4 dB across E-band. The pump configuration was selected to prioritize O- and E- band signal power. Additional pumps, both below 1220 nm and between the signal bands that would typically benefit ESCLU-band signals, were also tested but observed to strongly deplete the O-band and thus left as an avenue of future study on longer links.

Figure 8(b) shows the summary of signal quality measurements after 50 km transmission with the GMI and decoded data-rate for the measured 1505 channels covering 37.6 THz bandwidth. The highest data-rates were achieved in C-band where most components were designed for, and the lowest NF amplifiers were available. However, data-rates exceeding 250 Gb/s were achieved for most ESCL-band channels with only a small reduction to around 200-250 Gb/s for U-band channels. The high fiber loss and limited Raman gain meant that O-band channel data-rates were between 150 Gb/s and 200 Gb/s across the majority of the amplifier pass-band. Some variation in data-rate can also be observed due to the failure of auto-bias circuitry to operate in this region. The combined OESCLU-band date-rate after decoding was 378.9 Tb/s with the GMI estimated data-rate reaching 402.2 Tb/s, showing the potential for exceeding 400 Tb/s in a standard fiber with a sufficiently optimized coding scheme and the potential for a significant increase in optical fiber transmission capacity. We note that the 50 km transmission results show not dissimilar data rates to those measured in B2B, showing that the 50 km transmission system is largely transceiver limited. This could be expected from inspection of Fig. 8 (a), that shows a maximum span loss of 12 dB for SCLU-bands. Further, whilst the O-band span loss reaches 18 dB, the higher O and E-band loss is partially compensated for by distributed Raman amplification. Hence, the power into the post fiber amplifiers is sufficient to maintain reasonable noise performance. The similarity of B2B and 50 km data rates further suggests that the relatively low per-channel launch power means the impact of fiber non-linearities (aside from the SRS evident in fig. 8 (a) is low.

B. 100 km transmission and comparison

The characteristics of the Raman amplified 100 km fiber span are shown in Fig. 9 (a). The launched OESCLU-band input signal (red) becomes tilted at the fiber output (black) by the combination of SRS and wavelength dependent loss (dashed grey, right-axis). The addition of the Raman pumps provided gain across O-band to partially compensate for the higher fiber loss and moderate launch power. The Raman pumps between E- and O-bands provided some gain for E-band channels at the cost of slightly reducing the O-band Raman gain from increased SRS to the higher power E-band channels. We note that higher gain is evident after 100 km transmission despite the same pump power being used in both cases. This is attributed to gain saturation in the case of 50 km transmission where the signal power is higher in the region close to the counter propagating pumps than in the 100 km case. Further, for the E- and O-band signals comparatively more power is lost to higher wavelength channels through SRS in the 100 km case.

Figure 9 (b) shows the summary of signal quality measurements with the GMI and decoded data rates vs. wavelength. The highest data rate channels are in the C- and L-band where the fiber loss was lowest, and the spectral region is the one for which most components and modulators were designed. Lower data rates are observed at the edges of the DFA gain profiles and a slope across S-, C- and L-bands matching the increasing fiber attenuation can be observed. This is not seen for E-band channels that experienced some Raman gain. O-band channels showed significantly lower data rate channels that is partly a result of the higher fiber loss and moderate launch power in addition to the bias issues and high-loss of the C-band specified modulator described previously. The combined data rate of all 1440 WDM channels was 339.1 Tb/s when estimated from the GMI and 322.8 Tb/s after LDPC decoding.

Table 1 shows the number of channels and GMI data rate of each band for this 100 km measurement and the previous 50 km measurement for comparison. The impact of the fiber loss and lower input power to the first stage receiver amplifiers led to reduced data-rates for all channels. In all bands except C-band, the additional loss led to lower power into the 1st stage receiver amplifiers, also meaning that fewer edge channels, which typically see lower amplifier gain, could be recovered. The E, C and L-bands all showed similar reduction in data-rate of 13 %, 12% and 13% respectively from the extended transmission distance and were able to support a similar number of channels at both distances. In contrast, without any distributed Raman gain, the lower TDFA gain and higher NF at lower wavelengths lead to a reduced number of S-band channels, lowering the data-rate by over 27%. Similarly, fewer edge channels on the O-band could be received and combined with the limited launch power and high attenuation; this led to high receiver noise and 22% lower data-rate at the longer distance. The U-band demonstrated 33% data-rate reduction which was in part due to the large fiber loss at the longest wavelengths and the limited gain of discrete Raman amplifiers at shorter wavelengths. This led to an inverse U-shaped profile evident in Fig. 9(b). We note that the large variation in signal quality over the multi-band system could be suitable for FEC gain sharing as discussed for SDM systems in [41].

V. CONCLUSION

We have constructed a novel transmission system covering each of the major transmission bands in the low-loss window of silica optical fibers. The system uses a combination of 6 doped fiber amplifiers, discrete and distributed Raman amplification and utilizing some custom E- and O-band optical processors for spectrum flattening to support 25-GHz-spaced data channels

from 1281.2nm to 1649.9 nm. After amplifier and back-to-back transceiver characterization, for 50 km transmission, we report a GMI data-rate of 402.2 Tb/s and decoded data-rate of 378.9 Tb/s. This data-rate and aggregate transmission bandwidth of 37.6 THz both exceed those previously reported in SMF by 25% and 35% respectively. We then extend the transmission distance to 100 km, reporting a data-rate of 339.1 Tb/s (GMI) and 322.8 Tb/s after decoding but observing larger reductions for bands with higher fiber loss. Overall, these results show the potential of multi-band transmission to increase the information carrying capability of new and deployed optical fibers, whilst revealing the challenge of overcoming the high fiber loss of O- and U-bands in longer fiber spans.

ACKNOWLEDGMENT

We thank Ralf Stolte of Finisar for loan of U-band Waveshaper (profile shaping) and O-band Waveshaper (Rx filter). This work is supported by EPSRC Grant EP/V000969/1, EP/R035342/1 and Royal Society grant IES\R3\223001.

REFERENCES

[1] "Cisco Annual Internet Report - Cisco Annual Internet Report (2018–2023) White Paper - Cisco." https://www.cisco.com/c/en/us/solutions/collateral/executive-perspectives/annual-internet-report/white-paper-c11-741490.html (accessed Apr. 13, 2023).

[2] United Nations Conference on Trade and Development, Digital economy report 2019: value creation and capture: implications for developing countries. 2019.

[3] A. Ferrari, A. Napoli, N. Costa, J. K. Fischer, J. Pedro, W. Forysiak, A. Richter, E. Pincemin, and V. Curri, "Multi-Band Optical Systems to Enable Ultra-High Speed Transmissions," in 2019 Conference on Lasers and Electro-Optics Europe and European Quantum Electronics Conference, paper ci_2_3..

[4] J. K. Fischer et al., "Maximizing the Capacity of Installed Optical Fiber Infrastructure Via Wideband Transmission," in 2018 20th International Conference on Transparent Optical Networks (ICTON), Jul. 2018, pp. 1–4. doi: 10.1109/ICTON.2018.8473994.

[5] D. J. Richardson, J. M. Fini, and L. E. Nelson, "Space-division multiplexing in optical fibres," Nat. Photonics, vol. 7, no. 5, pp. 354–362, Apr. 2013, doi: 10.1038/nphoton.2013.94.

[6] B. J. Puttnam, G. Rademacher, and R. S. Luís, "Space-division multiplexing for optical fiber communications," Optica, vol. 8, no. 9, p. 1186, Sep. 2021, doi: 10.1364/OPTICA.427631.

[7] F. Poletti et al., 'Towards high-capacity fibre-optic communications at the speed of light in vacuum', Nat. Photonics, vol. 7, no. 4, pp. 279–284, Apr. 2013, doi: 10.1038/nphoton.2013.45.

[8] M. Ionescu, L. Galdino, A. Edwards, J. James, W. Pelouch, E. Sillekens, D. Semrau, D. Lavery, R. I. Killey, S. Barnes, P. Bayvel, S. Desbruslais. "91 nm C+L Hybrid Distributed Raman–Erbium-Doped Fibre Amplifier for High Capacity Subsea Transmission," 2018 European Conference on Optical Communication (ECOC), Rome, Italy, 2018, pp. 1-3, doi: 10.1109/ECOC.2018.8535151

[9] J. Renaudier, A. Arnould, D. Le Gac, A. Ghazisaeidi, P. Brindel, M Makhsiyan, A. Verdier, K. Mekhazni, F. Blache, H. Debregeas, A. Boutin, N Fontaine, D Neilson, R. Ryf, H. Chen, M. Achouche and G. Charlet '107 Tb/s Transmission of 103-nm Bandwidth over 3×100 km SSMF using Ultra-Wideband Hybrid Raman/SOA Repeaters', In Proc. Optical Fiber Communication Conference (OFC) 2019, paper Tu3F.2.1

[10] L. Galdino, A. Edwards, W. Yi, E. Sillekens, Y. Wakayama, T. Gerard, W. Sheldon Pelouch, S. Barnes, T. Tsuritani, R. I. Killey, D . Lavery and P. Bayvel 'Optical Fibre Capacity Optimisation via Continuous Bandwidth Amplification and Geometric Shaping', EEE Photonics Technology Letters, vol. 32, no. 17, pp. 1021-1024, 1 Sept.1, 2020, doi: 10.1109/LPT.2020.3007591.

[11] B. J. Puttnam, R. S. Luís, G. Rademacher, M. Mendez-Astudilio, Y. Awaji, and H. Furukawa, "S, C and Extended L-Band Transmission with Doped Fiber and Distributed Raman Amplification," in 2021 Optical Fiber Communications Conference and Exhibition (OFC), paper Fb3.3

[12] F. Hamaoka, M. Nakamura, M. Takahashi, T. Kobayashi, Y. Miyamoto, and Y. Kisaka, '173.7-Tb/s Triple-Band WDM Transmission using 124-Channel 144-GBaud Signals with SE of 9.33 b/s/Hz', in 2023 Optical Fiber Communications Conference and Exhibition (OFC), San Diego, CA, USA: IEEE, Mar. 2023, pp. 1–3. doi: 10.23919/OFC49934.2023.10116265.

[13] Y. Frignac et al., 'Record 158.4 Tb/s transmission over 2x60 km field SMF using S+C+L 18Thz-bandwidth lumped amplification', in 49th European Conference on Optical Communications (ECOC 2023), Oct. 2023, pp. 550–553. doi: 10.1049/icp.2023.2242.

[14] B. J. Puttnam, R. S. Luís, G. Rademacher, M. Mendez-Astudillio, Y. Awaji, and H. Furukawa, "S-, C- and L-band transmission over a 157 nm bandwidth using doped fiber and distributed Raman amplification," Opt. Express, vol. 30, no. 6, p. 10011, Mar. 2022, doi: 10.1364/OE.448837.

[15] X. Zhao, S. Escobar-Landero, D. Le Gac, A. Lorences-Riesgo, T. Viret-Denaix, Q. Guo, L. Gan, S. Li, S. Cao, X. Xiao, N. E. Dahdah, A. Gallet, S. Yu, H. Hafermann, L. Godard, R. Brenot, Y. Frignac, and G. Charlet, "2005 Tb/s Transmission with S+C+L Amplification Covering 150 nm Bandwidth over 2×100 km PSCF Spans," in European Conference on Optical Communication (ECOC) 2022, paper Th3C.4.

[16] D. Soma et al., "25-THz O+S+C+L+U-Band Digital Coherent DWDM Transmission Using a Deployed Fibre-Optic Cable" In Proc. European Conference on Optical Communication (ECOC) 2023, paper Th.C.2.4.

[17] B. J. Puttnam et al., "301 Tb/s E, S, C+L-Band Transmission over 212 nm bandwidth with E-band Bismuth-Doped Fiber Amplifier and Gain Equalizer" In Proc. European Conference on Optical Communication (ECOC) 2023 paper Th.C.2.4.

[18] B. J. Puttnam et al., '264.7 Tb/s E, S, C + L-Band Transmission over 200 km' Submitted to Optical Fiber Conference 2024, paper M1F.4

[19] B. J. Puttnam et al., '402 Tb/s GMI Data-Rate OESCLU-Band Transmission', Opt. Fiber Commun. Conf., 2024.

[20] B. J. Puttnam et al., '339.1 Tb/s OESCLU-band transmission over 100 km SMF' 50th European Conference on Optical Communications (ECOC 2024), Paper M.2.2

[21] B. J. Puttnam et al., '321 Tb/s E/S/C/L-band Transmission with E-band Bismuth-Doped Fiber Amplifier and Optical Processor', J. Light. Technol., pp. 1–8, 2024, doi: 10.1109/JLT.2024.3379676.

[22] 'Amonics Product Catalog System'. Accessed: Nov. 17, 2024. [Online]. Available: https://www.amonics.com/product/5 Accessed 17/11/24

[23] M. J. Andrejco, I. P. Byriel, and B. Palsdottir, 'Erbium doped fibers for extended L-band amplification', US6560009B1, May 06, 2003 https://patents.google.com/patent/US6560009B1/en Accessed 17/11/24

[24] 'Fluoride Fiber - FiberLabs Inc.', FiberLabs Inc. - Specialty Fiber Amplifiers and Fluoride Fibers. Accessed: Jun. 17, 2024. [Online]. Available: https://www.fiberlabs.com/glossary/fluoride-fiber/

[25] TDFA characteristics Accessed: Jun. 17, 2024. [Online]. Available: https://www.fiberlabs.com/bt_amp_index/s-band-bt-amp/

[26] Y. Wang, N. K. Thipparapu, D. J. Richardson and J. K. Sahu, "Ultra-Broadband Bismuth-Doped Fiber Amplifier Covering a 115-nm Bandwidth in the O and E Bands," in Journal of Lightwave Technology, vol. 39, no. 3, pp. 795-800, 1 Feb.1, 2021, doi: 10.1109/JLT.2020.3039827.

[27] A. Donodin et al., 'Bismuth doped fibre amplifier operating in E- and S-optical bands', Opt. Mater. Express, vol. 11, no. 1, p. 127, Jan. 2021, doi: 10.1364/OME.411466.

[28] Y. Ososkov, A. Khegai, S.Firstov, K. Riumkin, S. Alyshev, Alexander Kharakhordin, A. Lobanov, A. Guryanov, and M. Melkumov, "Pump-efficient flattop O+E-bands bismuth-doped fiber amplifier with 116 nm – 3 dB gain bandwidth," Opt. Express 29, 44138-44145 (2021)

[29] N. Taengnoi, K. R. H. Bottrill, Y. Hong, L. Hanzo, and P. Petropoulos, 'Ultra-Long-Span U-Band Transmission Enabled by Incoherently Pumped Raman Amplification', J. Light. Technol., vol. 41, no. 12, pp. 3767–3773, Jun. 2023, doi: 10.1109/JLT.2023.3265172.

[30]

[31] M. Tan et al., 'RIN Mitigation and Transmission Performance Enhancement With Forward Broadband Pump', IEEE Photonics Technol. Lett., vol. 30, no. 3, pp. 254–257, Feb. 2018, doi: 10.1109/LPT.2017.2784480.

[32] M. A. Iqbal, M. Tan, and P. Harper, 'Enhanced Transmission Performance Using Backward-Propagated Broadband ASE Pump', IEEE Photonics Technol. Lett., vol. 30, no. 9, pp. 865–868, May 2018, doi: 10.1109/LPT.2018.2821191.

[33] D. Pratiwi, D. Orsuti, M. Tan, B. J. Puttnam, R. S. Luis, A. Donodin, I. Phillips, L. Palmieri, H. Furukawa, W. Forysiak 'Gain Incoherently Pumped Discrete Raman Amplifiers for U-band Coherent Transmission Systems'

[34] S. Liang et al., '102-nm-wide, high-gain, low-noise lumped Raman amplifier', in 49th European Conference on Optical Communications (ECOC 2023), Oct. 2023, pp. 632–635. doi: 10.1049/icp.2023.2274.

[35] N. K. Fontaine, I. D. Phillips, W. Forysiak, L Dallachiesa, M. Mazure, R, Ryf, H, Chen and D, T. Nielson, "Multiport E-band Wavelength equalizer," in 2023 European Conference on Optical Communication (ECOC), paper P86

[36] D.J. Elson, G. Saavedra, K. Shi, D. Semrau, L. Galdino, R. Killey, B. C. Thomsen, and P. Bayvel, "Investigation of bandwidth loading in optical fibre transmission using amplified spontaneous emission noise," Opt. Express 25, 19529-19537 (2017)

[37] H. Buglia, E. Sillekens, A. Vasylchenkova, P. Bayvel, and L. Galdino, 'On the impact of launch power optimization and transceiver noise on the performance of ultra-wideband transmission systems [Invited]', *J. Opt. Commun. Netw.*, vol. 14, no. 5, pp. B11–B21, May 2022, doi: 10.1364/JOCN.450726.

[38] J. Cho, L. Schmalen, and P. J. Winzer, 'Normalized Generalized Mutual Information as a Forward Error Correction Threshold for Probabilistically Shaped QAM', in 2017 European Conference on Optical Communication (ECOC), Sep. 2017, pp. 1–3. doi: 10.1109/ECOC.2017.8345872.

[39] A. Alvarado, E. Agrell, D. Lavery, R. Maher and P. Bayvel, "Replacing the Soft-Decision FEC Limit Paradigm in the Design of Optical Communication Systems," in *Journal of Lightwave Technology*, vol. 34, no. 2, pp. 707-721, 15 Jan.15, 2016, doi: 10.1109/JLT.2015.2482718

[40] R. S. Luís et al., 'Experimental Demonstration of a Petabit per Second SDM Network Node', J. Light. Technol., vol. 38, no. 11, pp. 2886–2896, Jun. 2020, doi: 10.1109/JLT.2020.2988886.

[41] B. J. Puttnam et al., 'High Capacity Transmission Systems Using Homogeneous Multi-Core Fibers', J. Light. Technol., vol. 35, no. 6, pp. 1157–1167, Mar. 2017, doi: 10.1109/JLT.2017.2669207.